

INFORMATION TO USERS

This manuscript has been reproduced from the microfilm master. UMI films the text directly from the original or copy submitted. Thus, some thesis and dissertation copies are in typewriter face, while others may be from any type of computer printer.

The quality of this reproduction is dependent upon the quality of the copy submitted. Broken or indistinct print, colored or poor quality illustrations and photographs, print bleedthrough, substandard margins, and improper alignment can adversely affect reproduction.

In the unlikely event that the author did not send UMI a complete manuscript and there are missing pages, these will be noted. Also, if unauthorized copyright material had to be removed, a note will indicate the deletion.

Oversize materials (e.g., maps, drawings, charts) are reproduced by sectioning the original, beginning at the upper left-hand corner and continuing from left to right in equal sections with small overlaps.

ProQuest Information and Learning
300 North Zeeb Road, Ann Arbor, MI 48106-1346 USA
800-521-0600

UMI[®]

Optimal and Intelligent Multi-Axis CNC Tool Path Generation for Sculptured Part Machining

by

Zezhong Chevy Chen


B. Eng., Beijing University of Posts and Telecommunications, 1989
M. A. Sc., Beijing University of Posts and Telecommunications, 1992

A Dissertation Submitted in Partial Fulfillment of the
Requirements for the Degree of

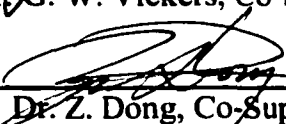
DOCTOR OF PHILOSOPHY

in the Department of Mechanical Engineering

We accept this dissertation as conforming
to the required standard




Dr. G. W. Vickers, Co-Supervisor (Department of Mechanical Engineering)



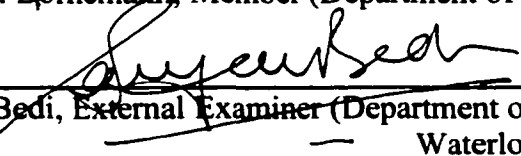
Dr. Z. Dong, Co-Supervisor (Department of Mechanical Engineering)



Dr. J. W. Provan, Member (Department of Mechanical Engineering)



Dr. J. Bornemann, Member (Department of Electrical and Computer Engineering)



Dr. S. Bedi, External Examiner (Department of Mechanical Engineering, University of
Waterloo)

© ZEZHONG CHEVY CHEN, 2002
University of Victoria

All rights reserved. This dissertation may not be reproduced in whole or in part, by
photocopy or other means, without the permission of the author.



**National Library
of Canada**

**Acquisitions and
Bibliographic Services**

**395 Wellington Street
Ottawa ON K1A 0N4
Canada**

**Bibliothèque nationale
du Canada**

**Acquisitions et
services bibliographiques**

**395, rue Wellington
Ottawa ON K1A 0N4
Canada**

Your file / Votre référence

Our file / Notre référence

The author has granted a non-exclusive licence allowing the National Library of Canada to reproduce, loan, distribute or sell copies of this thesis in microform, paper or electronic formats.

The author retains ownership of the copyright in this thesis. Neither the thesis nor substantial extracts from it may be printed or otherwise reproduced without the author's permission.

L'auteur a accordé une licence non exclusive permettant à la Bibliothèque nationale du Canada de reproduire, prêter, distribuer ou vendre des copies de cette thèse sous la forme de microfiche/film, de reproduction sur papier ou sur format électronique.

L'auteur conserve la propriété du droit d'auteur qui protège cette thèse. Ni la thèse ni des extraits substantiels de celle-ci ne doivent être imprimés ou autrement reproduits sans son autorisation.

0-612-74931-2

Canada

Supervisors: Drs. Geoffrey W. Vickers and Zuomin Dong

Abstract

The main objective of tool path planning for sculptured part finishing is to attain the required surface-quality and maximum machining efficiency concurrently. This work addresses these challenging and conflicting tasks that demand more research.

The study identifies and mathematically proves a new tool path planning principle for 3-axis sculptured part machining - a steepest-directed tool path is the most efficient tool path scheme for a single tool path. An innovative tool path generation method, integrated steepest-directed and iso-cusped (SDIC) approach, is proposed for 3-axis sculptured part finishing. In this approach, the steepest-directed tool paths form a frame that controls the tool path directions for higher machining efficiency, and the iso-cusped tool paths fill this frame to prevent redundant tool motions and to ensure adequate surface quality. A hemi-cylindrical part is used to illustrate this approach and to demonstrate its superiority.

To machine complex sculptured surfaces that usually require expensive 5-axis machining, a cost-effective $3\frac{1}{2}\frac{1}{2}$ -axis machining scheme is discussed. The $3\frac{1}{2}\frac{1}{2}$ -axis machining is carried out by rotating the part to the cutter/part orientations that are defined by subdivided surface patches, discretely and sequentially using a tilt-rotary table attached to the 3-axis CNC machine. Under each orientation, the corresponding surface patch is machined using effective 3-axis CNC tool paths, i.e. the SDIC scheme. A method that automatically generates effective tool paths to facilitate the $3\frac{1}{2}\frac{1}{2}$ -axis machining is introduced. This approach optimizes the subdivision of a complex sculptured surface based on surface geometry and identifies the favourable cutter/part orientation for each subdivided surface patch, using fuzzy pattern recognition and Voronoi diagram. The advantages of this approach are demonstrated through a benchmark example.

This work contributes to the automated and optimal CNC tool path generation for sculptured part machining and has potential to benefit the aeronautic, automotive and die/mould manufacturing industries.

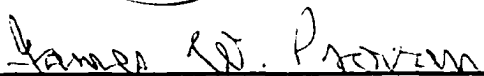
Examiners:



Dr. G. W. Vickers, Co-Supervisor (Department of Mechanical Engineering)



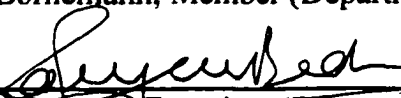
Dr. Z. Dong, Co-Supervisor (Department of Mechanical Engineering)



Dr. J. W. Provan, Member (Department of Mechanical Engineering)



Dr. J. Bornemann, Member (Department of Electrical and Computer Science)



Dr. S. Bedi, External Examiner (Department of Mechanical Engineering, University of Waterloo)

Table of Contents

Abstract	ii
Table of Contents	iv
List of Tables	vii
List of Figures	xiii
Acknowledgement	x
Chapter 1 Introduction	1
1.1 Sculptured Parts	1
1.2 CAD/CAE/CAM of Sculptured Parts	3
1.3 CNC Machining of Sculptured Parts	5
1.3.1 Two-and-a-Half-Axis CNC Machining	7
1.3.2 Three-Axis CNC Machining	7
1.3.3 Five-Axis CNC Machining	9
1.4 Related Work on CNC Tool Path Generation	12
1.4.1 Two-and-a-Half-Axis CNC Tool Path Generation Methods	12
1.4.2 Three-Axis CNC Tool Path Generation Methods	12
1.4.3 Five-Axis CNC Tool Path Generations	15
1.5 Outline of this Dissertation	17
Chapter 2 Measure of Machining Efficiency - Effective Cutting Edge	19
2.1 Terminology and Concepts in CNC Machining	19
2.2 Objectives of Tool Path Planning	21
2.3 Generic Machining Model	22
2.4 Steepest Tangent Direction on a Sculptured Surface at a Cutter Contact Point	24
2.5 Cutter and Surface Normal Expressions in Cutter Motion Frame	28
2.5.1 Cutter Geometry Frame (CGF)	28
2.5.2 Cutter Location Frame (CLF)	30
2.5.3 Steepest Direction Frame (SDF)	31
2.5.4 Cutter Motion Frame (CMF)	32

2.6	Planar Cutting Edge and Effective Cutting Edge	34
2.6.1	Planar Cutting Edge.....	34
2.6.2	Effective Cutting Edge	35
Chapter 3	Mathematic Proof on the Steepest Tangent Direction – the Most Efficient Tool Feed Direction in 3-Axis CNC Machining	37
3.1	Ball End-Mills Machining Efficiency Independent of the Tool Feed Direction ...	38
3.2	Most Efficient Tool Feed Direction for Flat End-Mill	39
3.3	Most Efficient Tool Feed Direction for Torus End-Mill	43
3.3.1	ECE Length ($L_{\alpha=0}$).....	44
3.3.2	ECE Length ($L_{\alpha=0}$) – Maximum of the ECE Lengths (L_{α}).....	48
3.4	An Example	50
Chapter 4	Steepest-Directed Tool Path – The Most Efficient Single Tool Path	54
4.1	Introduction.....	54
4.2	Steepest-Directed Tool Path	55
4.3	New Principle and Verification	57
4.3.1	New Principle in 3-Axis CNC Machining.....	57
4.3.2	ECE Length vs. Tool Feed Direction	58
4.4	Relationship between Machining Efficiency and Three Variables	60
Chapter 5	Integrated Steepest-Directed and Iso-Cusped (SDIC) Tool Paths	66
5.1	Introduction.....	66
5.2	Related Work	67
5.3	Steepest-Directed Method and Iso-Cusped Method.....	69
5.3.1	Steepest-Directed Tool Path	70
5.3.2	Iso-Cusped Tool Path	70
5.4	Integration of Steepest-Directed and Iso-Cusped Tool Paths.....	75
5.5	SDIC Tool Path Generation Procedure.....	76
5.6	SDIC Application	77
5.6.1	SDIC Tool Path Patterns.....	78
5.6.2	Optimum SDIC Tool Path	83
5.6.3	Sensitivity Study on SDIC Tool Paths.....	85
5.7	Machining Example for Comparison.....	89
5.7.1	Iso-Cusped, SDIC, and Steepest-Directed Tool Paths.....	89
5.7.2	Machining Results	92
Chapter 6	Automated Generation of Effective 3½/2-Axis CNC Tool Paths	95

6.1	Introduction.....	95
6.2	Comparison among 3, 5, and 3½½-Axis CNC Machining.....	97
6.3	Geometric Parameters and Machinability Parameters.....	101
6.3.1	Sculptured Surface Expression	101
6.3.2	Geometric Parameters.....	102
6.3.3	Machinability Parameters	104
6.4	Fuzzy Pattern Clustering Methods and Hierarchical Data Structure.....	106
6.5	Surface Feature Recognition with Hierarchical Data Structure	107
6.6	Subtractive Fuzzy Clustering and Fuzzy C-Means Methods	108
6.7	Voronoi Diagram for Surface Patch Boundaries	111
6.8	Part Orientation, Tool Path Planning, and Surface Machining	113
6.9	3½½-Axis CNC Programming Example	115
Chapter 7	Summary and Contributions	121
	Bibliography	123

List of Tables

Table 3.1 ECE Length along Different Tool Feed Directions for Different Cutters	53
Table 5.1 Cylinder Length vs. Length of SDIC Tool Paths.....	87
Table 5.2 Cylinder Radius vs. Length of SDIC Tool Paths.....	87
Table 5.3 Tool Radius vs. Length of SDIC Tool Paths.....	88
Table 5.4 Surface Tolerance vs. Length of SDIC Tool Paths.....	88
Table 6.1 Relationship between Gouging and Principal Curvatures	105
Table 6.2 Relationship between Surface Shape and Geometric Parameters.....	108

List of Figures

Figure 1.1 (a) Parametric Surface Patch; (b) Sculptured Surface of a Mouse	2
Figure 1.2 (a) Ferrari Formula One Racing Car; (b) Turbines of Airplane Engines.....	3
Figure 1.3 (a) 3D Solid Model of a Race Car; (b) Stress Distribution of a Pair of Gears; (c) Machining Simulation of a Handset Die	5
Figure 1.4 Three Types of Common Milling Cutters	6
Figure 1.5 Diagram of a 3-Axis CNC Vertical Milling Machine	8
Figure 1.6 Diagram of a 5-Axis CNC Milling Machine	10
Figure 1.7 Cutter/Part Reorientation by (a) Rotating Work Table; (b) Rotating Cutter ..	11
Figure 2.1 Iso-Cusped Tool Paths, Sculptured and Tolerance Surfaces	20
Figure 2.2 Three-Axis CNC Tool Path Diagram	21
Figure 2.3 Generic Machining Model of Sculptured Parts for Effective Cutting Edge...	23
Figure 2.4 Steepest Tangent Direction of a Surface at a CC Point	24
Figure 2.5 Torus End-mill in Cutter Geometry Frame and Cutter Location Frame	29
Figure 2.6 Torus End-mill Diagram.....	29
Figure 2.7 Cutter Location, Steepest Direction, and Cutter Motion Frames: (a) Frames at the CC point P_0 on the Surface; (b) Zoom-in Picture of the Frames.....	31
Figure 2.8 Effective Cutting Edge: (a) Cutter Mills a Surface; (b) Projection of Cutter on Cutting Edge Plane ($l-n$) along Tool Feed Direction (m)	35
Figure 2.9 Relationship between ECE and two factors (Free-formed Surface and Tolerance Surface).....	36
Figure 3.1 (a) Flat End-mill Machining Model; (b) Projection of Intersection Curve.....	41
Figure 3.2 (a) Intersection between the Cutting Surface and the Λ -offset plane Γ ; (b) Zoom-in View of the ECE from STD	44
Figure 3.3 View along n -axis on the Intersection Curve on Γ	45
Figure 3.4 ECE Length along the TFD, \mathbf{m}	49
Figure 3.5 Horizontal Cylinder and Tool Feed Directions.....	51
Figure 3.6 Machined Hemi-cylinder Part.....	52
Figure 4.1 Steepest-Directed Tool Path for a Sculptured Surface	56
Figure 4.2 Horizontal Cylinder and Tool Feed Directions.....	58

Figure 4.3 ECE Lengths of Three Cutters in Five Tool Feed Directions.....	60
Figure 4.4 Relationship between ECE Length and Tool Feed Direction at CC Point (80°, 50mm)	62
Figure 4.5 Relationship between ECE Length and Tool Feed Direction at CC Point (70°, 50mm)	63
Figure 4.6 Relationship between ECE Length and Tool Feed Direction at CC Point (60°, 50mm)	64
Figure 4.7 Relationship between ECE length and CC Points	65
Figure 5.1 Sculptured and Tolerance Surfaces with Tool Paths and Cusps.....	68
Figure 5.2 Iso-cusped Tool Paths of a Free-form Surface	71
Figure 5.3 Iso-Cusp Adjacent Point Calculation Algorithm	72
Figure 5.4 Integration of Steepest-Directed and Iso-Cusped Tool Paths.....	76
Figure 5.5 Horizontal Hemi-Cylinder and Flat End-milling Cutter.....	78
Figure 5.6 SDIC Tool Paths of the Hemi-cylinder Part	79
Figure 5.7 SDIC Tool Paths with a Frame of One Steepest-Directed Tool Path.....	81
Figure 5.8 SDIC Tool Paths with a Frame of Six Steepest-Directed Tool Paths.....	82
Figure 5.9 SDIC Tool Paths with a Frame of Fifty-two Steepest-Directed Tool Paths...	83
Figure 5.10 Curve of Tool Path Length vs. Number of Steepest-directed Tool Path	85
Figure 5.11 SDIC Tool Paths of the Half-Cylinder Part	90
Figure 5.12 SDIC Tool Paths with a Frame of One Steepest-Directed Tool Path.....	91
Figure 5.13 SDIC Tool Paths with a Frame of 33 Steepest-Directed Tool Paths	92
Figure 5.14 Three Types of Tool Paths for the Hemi-Cylindrical Part.....	93
Figure 5.15 SDIC Tool Path and a Machined Part with Surface Tolerance 0.01 mm.....	94
Figure 6.1 3½/2-Axis CNC Machining with a 3-Axis CNC Machine and a Tilt-Rotary Table	99
Figure 6.2 B-Spline Surface with Convex, Concave, and Saddle Shapes	102
Figure 6.3 Surface Grid Points and Their Cluster Centers.....	111
Figure 6.4 Voronoi Diagram on Thirty-Seven Sites and Regions	113
Figure 6.5 Optimal Part Set-up for a Surface Patch in the 3½/2-axis CNC Machining.	115

Figure 6.6 B-Spline Surface and its Control Polyhedron.....	116
Figure 6.7 Subtractive Fuzzy Clustering on Grid Points of the Surface	117
Figure 6.8 Fourteen Clusters by Fuzzy C-Means Clustering Method.....	118
Figure 6.9 Voronoi Diagram for the Subsurface Patch Boundaries.....	119
Figure 6.10 Surface Patches and Surface Normals at the Cluster Centres.....	120

Acknowledgement

Special thanks to my supervisors, Drs. Geoffrey W. Vickers and Zuomin Dong. I really appreciate their enlightenment, encourage, support, and trust in me. Thanks to Shigeng Wang for giving me a lot of advices and Gregery Balchin, Shari Yore, and Gene Racicot for proofreading my dissertation.

Victoria's mild weather, kind people, and quiet environment are also very helpful to my research.

This hard and fruitful Ph.D. program gears me up to my life goal – to pursue the best in the world.

Chapter 1 Introduction

1.1 Sculptured Parts

Sculptured parts are playing important roles in mechanical design in industry due to their geometric features. Sculptured parts are a type of mechanical parts with a curved shape represented by free-form surfaces. The free-form surface is defined mathematically as a collection of interconnected and bounded parametric patches through blending and interpolation [50]. Each parametric patch is formulated in a mathematic function with two parameters, e.g. t and s , ranging from zero to one (see Fig. 1.1(a) [20]). These parametric patches are classified into Bi-cubic, Bezier, Non-Uniform Rational B-Spline (NURBS), and Coons surfaces [20]. Because the parametric patches are in curved form, the sculptured surface is able to represent very complex shapes in design. A computer mouse in Fig. 1.1(b) is an example of a sculptured surface.

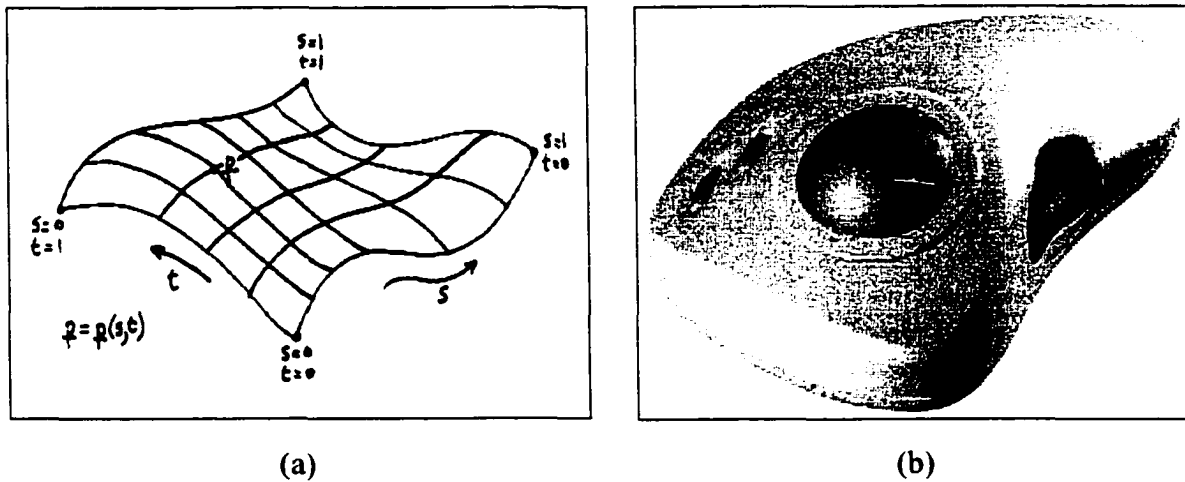


Figure 1.1 (a) Parametric Surface Patch; (b) Sculptured Surface of a Mouse

Unlike the prismatic parts, sculptured parts have an aesthetic appearance and can offer ergonomic, aerodynamic, or hydrodynamic functionality. Frequently used electronics (e.g., CD player, shaver, speaker, and joystick, etc.,) employ many sculptured parts for an appealing appearance. The injection mould to make these electronic parts should be sculptured. The body of the Ferrari-Formula-One racing car in Fig. 1.2(a) is designed with sculptured surfaces, as is the die for the sheet metal of the body. The turbine blades in airplane engines are an application of sculptured parts in the aeronautics industry (see Fig. 1.2(b)). These parts with aerodynamic shapes increase the efficiency of the engine. Sculptured parts are important parts in the aeronautical, automotive, and injection mould/die industries; therefore, their efficient design and manufacturing is profitable and in high demand.



Figure 1.2 (a) Ferrari Formula One Racing Car; (b) Turbines of Airplane Engines

1.2 CAD/CAE/CAM of Sculptured Parts

Because of the complex shape of sculptured parts, they demand advanced computer-aided technology in their design and manufacturing, rather than traditional methods for the prismatic parts. Studies have shown that computer aided design, computer aided engineering, and computer aided manufacturing (CAD/CAE/CAM) are a satisfactory method to design and manufacture sculptured parts efficiently and precisely.

Efficient design and manufacturing of sculptured parts demand technical advances in several related fields. These fields include:

- building 3D sculptured surface models and the assembly with sculptured parts,
- finite element analysis (FEA) and computational fluid dynamics (CFD),
- multi-axis CNC tool path generation and machining simulation,
- multi-axis CNC milling machines and the cutters, and
- scanning for the part surface inspection.

Meanwhile, sculptured part design, analysis, machining, and inspection should be networked so that the information at each stage is shared and problems can be quickly identified and solved. The demands of sculptured parts however can not be met by blueprint design, hand calculation, manually-operated machines, and mechanical calibers for inspection.

CAD/CAE/CAM technology is a perfect fit for the design and manufacturing requirements of sculptured parts. A feature-based, parametric solid modeller in the CAD module can deal with complex surfaces. A 3D solid model of a race car with a sculptured body is shown in Fig. 3(a). The FEA and CFD carried out in the CAE module provide necessary analysis to ensure the part performs properly. For example, the stress distribution of a pair of working gears can be calculated and displayed using the FEA method (see Fig. 3(b)). Since sculptured parts are machined on multi-axis CNC machine tools, the tool paths are generated automatically in the CAM module. Also the CAM module can simulate the CNC machining process to verify the tool paths. Fig. 3(c) shows a cutter machining the die of a handset along the tool paths in a CNC machining simulation. Being the main tool in manufacturing, the precise CNC machines cut the parts to the specified surface tolerance accurately; and the laser scanning tools inspect the machined surface quality. Without CAD/CAE/CAM technology, sculptured parts can not be designed with an appealing appearance and made with required fluid dynamic properties; not to mention their wide industrial applications.

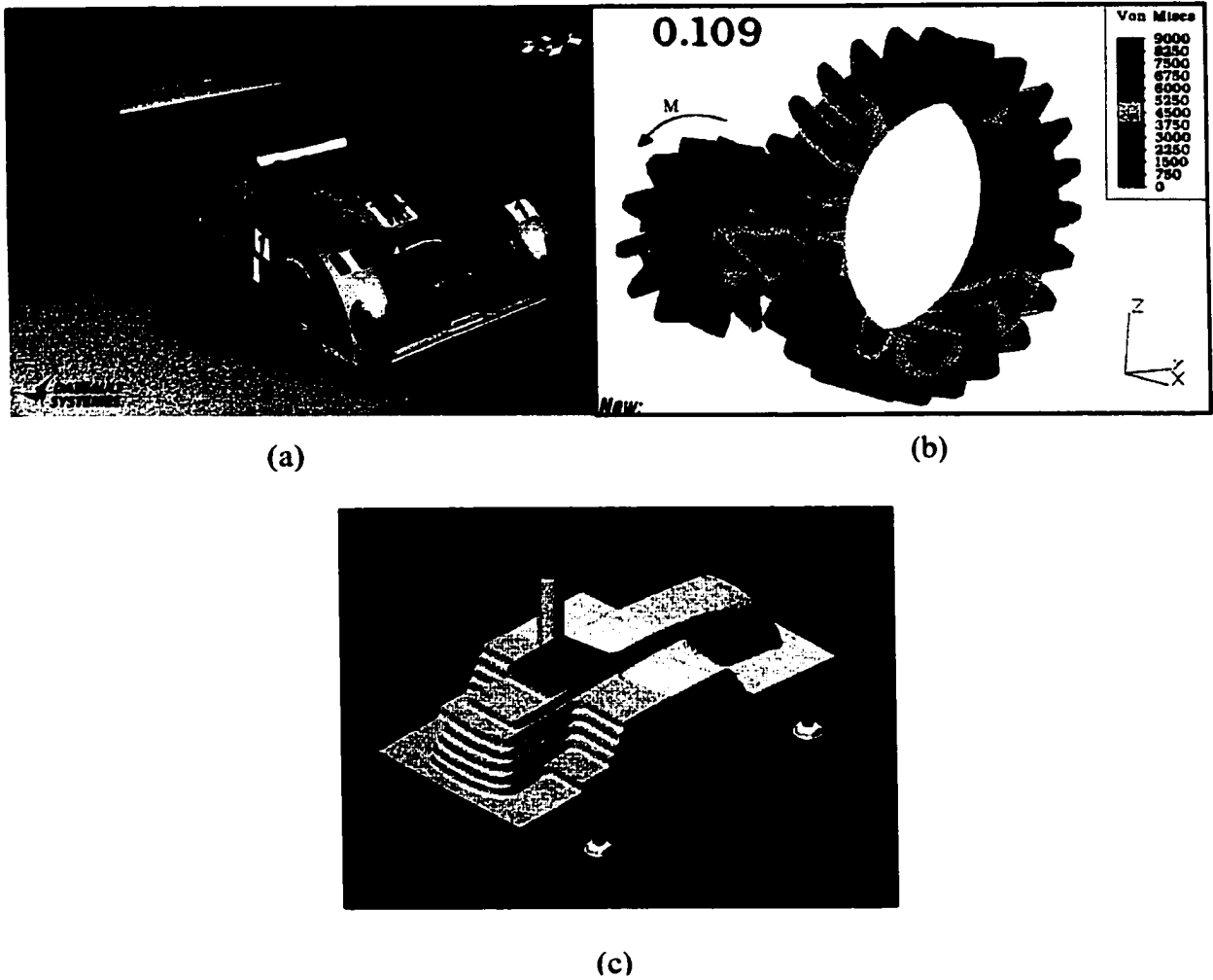


Figure 1.3 (a) 3D Solid Model of a Race Car; (b) Stress Distribution of a Pair of Gears; (c) Machining Simulation of a Handset Die

1.3 CNC Machining of Sculptured Parts

The machining of a sculptured part consists of three steps: (1) rough machining, (2) semi-finish and finishing machining, and (3) grinding/polishing. Rough machining removes the excess stock material quickly just to form a shape slightly larger than the part design, thus high machining productivity is its primary concern. Finishing machining produces adequate-quality surfaces by cutting the rough shape to the design. Better surface

finishing requires less costly and labour-intensive manual polishing at the final stage. Adequate-quality surfaces, less gouging, and minimum machining time are the objectives of the finishing machining. Different machining strategies and tool path patterns lead to variations in machining productivity and surface quality. A balance between tool paths and the machining time can be achieved by optimizing the 3-axis CNC tool paths.

Most sculptured parts are currently machined with CNC machine tools. These machines are classified into three types: 2½-axis, 3-axis, and 5-axis CNC machines. The cutter on these machines includes three common types: ball, torus, and flat end-mill (see Fig. 1.4). According to the different objectives of the rough and finishing machining, normally 2½-axis CNC machines are used for the rough machining, and 3-axis and 5-axis CNC machines are used for the finishing machining. In this section, the features of the three types of machines are introduced; and the principles of selecting a CNC machine for sculptured part machining are discussed.

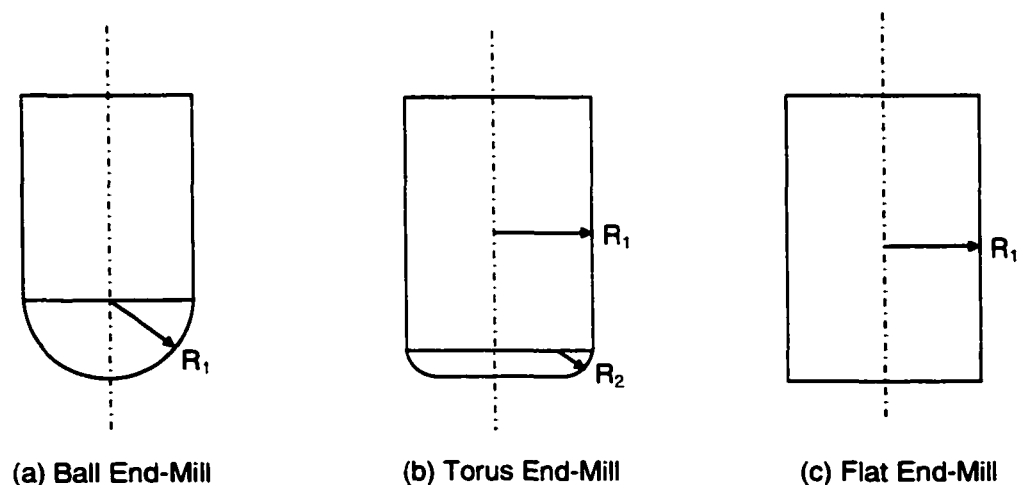


Figure 1.4 Three Types of Common Milling Cutters

1.3.1 Two-and-a-Half-Axis CNC Machining

Two-and-a-half-axis CNC machining is often used for rough machining [17]. The main feature of this type of machining is that the cutter motion in Z direction is not synchronized with the worktable motion in X and Y direction, in other words, the cutter remains the same height in Z direction when it cuts on a layer parallel to the worktable (X-Y plane). For the term 2½-axis CNC machining, “2” means the X- and Y-axis motions, and “½” means the Z-axis motion. Most of the 2½-axis CNC machining is carried out on 3-axis CNC milling machines.

Two-and-a-half-axis CNC machining is very efficient due to the highest material removal rate of the cutter and the rigid setup. Several parallel layers are made to generate part contours. The cutter executes the plane milling to remove the stock material according to the contour in a layer, and the plane milling is carried on all layers. A terrace-shaped part is generated to approximate the design part. Since plane machining is more efficient than contour machining, this machining strategy is quick in roughly shaping the surface. However, the terrace-shaped part has larger surface roughness than the specified surface tolerance; and this machining is not applicable to the finishing machining of sculptured parts.

1.3.2 Three-Axis CNC Machining

Three-axis CNC machines are quite popular in the manufacturing industry due to their features, their advantages and high industrial demand. Three-axis CNC machining is exerted when a cutter of a 3-axis CNC machine moves along planned tool paths. This is because a 3-axis CNC machine executes three simultaneous

motions including motions of the working table along X- and Y-axis and the cutter motion along Z-axis. Determined by the machine's architecture, the main feature of the machine is that the cutter orientation with respect to the part is locked after the part is fixed on the worktable. A 3-axis CNC vertical milling machine is shown in Fig. 1.5; the cutter orientation is always in the vertical direction.

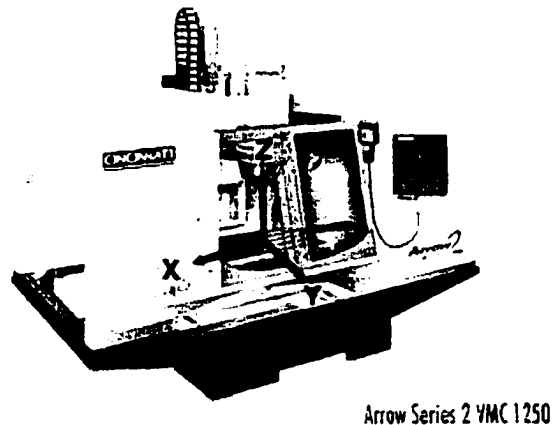


Figure 1.5 Diagram of a 3-Axis CNC Vertical Milling Machine

Compared with 5-axis CNC machining, the 3-axis CNC machining strategy enjoys some advantages. These advantages generally are (a) the machine is affordable even for small businesses and its maintenance is not expensive; (b) higher stiffness and rigidity of the machine prevents chatter in machining; (c) machine accuracy is high enough for finishing machining; and (d) programming for tool paths in 3-axis CNC machining is manageable. Moreover, 3-axis CNC machining is the main metal working strategy in the production process. Statistics show that besides the accurate prismatic parts, a majority of sculptured parts in the die/mould industry

are made with 3-axis CNC machines. Therefore, 3-axis CNC machining is a major force in manufacturing industry.

Despite the popularity of 3-axis CNC machines, they are not universally able to mill all parts. If the cutter can not access some surface regions (or surface patches) of a sculptured part without interfering it, these surface patches are called the *occult surface patches* in this set-up. Three-axis CNC machines can not be applied to this part. On the other hand, a principle of choosing 3-axis CNC machining for sculptured parts is that all surface patches to be machined in the sculptured part should be accessible by the cutter in the part set-up. For sculptured parts with occult surface patches, a feasible solution to machining the parts is 5-axis CNC machining.

1.3.3 Five-Axis CNC Machining

For decades, 5-axis CNC machining has been synonymous with sculptured parts with occult surface patches, because the simultaneous movement of five machine axes is required to cut the occult surface patches. A majority of the 5-axis CNC technology users are large companies in the aerospace, automotive, and aircraft industries.

The mechanism of 5-axis CNC machines provides the simultaneous five axes movement in this way. A 5-axis CNC machine has three linear X-, Y-, and Z-axis motions (identical to a 3-axis CNC machine) and two A- and B-axis rotations along two of the X-, Y-, and Z-axis, respectively (Some configurations are invalid for 5-axis CNC machines [41]). Because the rotations are synchronized with the linear motions, “5-axis” refers to X-, Y-, Z-, A-, and B-axis. In Figure 1.6, a 5-axis CNC milling

machine is shown, and the cutter tilts in and out for the A-axis and pivots left and right for the B-axis.

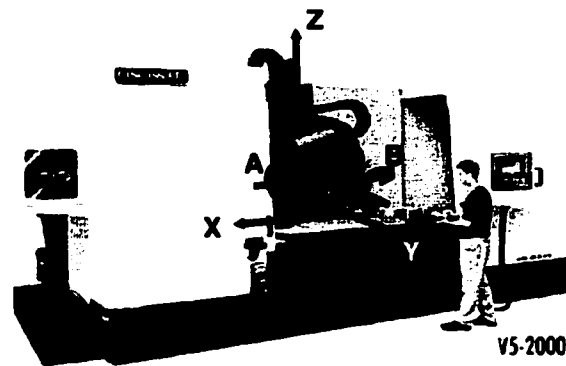


Figure 1.6 Diagram of a 5-Axis CNC Milling Machine

The function of the rotating axes is to change the cutter orientation with respect to the sculptured part without resetting up the part, so that the cutter can access the occult surface patches of the part. Current machines carry out the rotations either by rotating the working table along X- and Y-axis, which is not horizontal as shown in Fig. 1.7(a), or by swinging back and forth and left and right, shown in Fig. 1.7(b). With the two rotating axes, A and B, the cutter is able to alter its orientation to access and machine the occult surface patches without gouging and collision between the part and the cutter.

Five-axis CNC machines have the advantage of stronger manufacturing capability. The advantages of 5-axis CNC machines include (a) increased part-making diversity and the ability to make complex parts more efficiently, (b) increased productivity throughout by eliminating part set-ups and handlings, (c) reduced in-process inventory costs while raising just-in-time part scheduling, (d) optimum part

quality and accuracy while reducing scrap and rework, (e) lowered door-to-door manufacturing costs by cutting the number of machines in the manufacturing chain, and (f) lowered fixture cost and the number of dedicated fixtures and tools. However, 5-axis CNC machining has not yet been widely applied by industry because of its high investment, costly maintenance, less rigid, chatter-prone machine tool structure, and the need for experienced programmers to generate complex 5-axis tool paths.

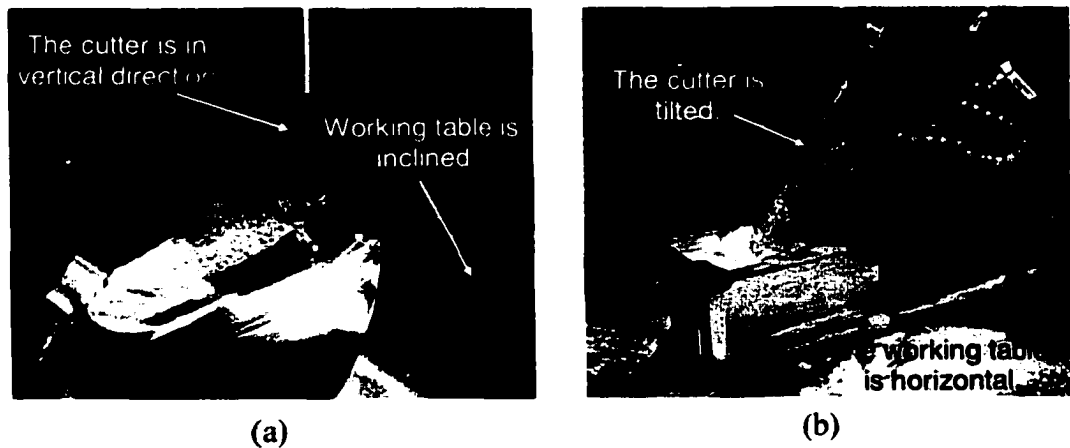


Figure 1.7 Cutter/Part Reorientation by (a) Rotating Work Table; (b) Rotating Cutter

Due to the different characteristics of the three stated CNC machining methods, the tool path generation approaches for them are different. The following section provides a literature review on CNC tool path generation methods.

1.4 Related Work on CNC Tool Path Generation

1.4.1 Two-and-a-Half-Axis CNC Tool Path Generation Methods

Two-and-a-half-axis CNC machining with flat end-mills is efficient in sculptured part rough machining, as mentioned before. Well-planned tool paths in each layer can further improve machining efficiency. Extensive research has been carried out on 2½-axis CNC tool path generation for rough machining of sculptured parts, including the work done at the University of Victoria [17].

This study covers machining strategy planning, optimal tool path patterns identification, and machining parameter optimization. To generate tool paths for each layer and determine the distance between two layers, mathematical modeling, fuzzy pattern identification, and optimization have been used. It also incorporates qualitative production knowledge and quantitative machine shop data into the tool path planning. The cutter feed rate and spindle rate are adjusted to optimum, based on the on-line prediction of cutting forces. A significant improvement on machining productivity has been achieved. However, the 2½-axis CNC machining scheme can not be used in finishing machining of sculptured parts.

1.4.2 Three-Axis CNC Tool Path Generation Methods

For 3-axis CNC sculptured part machining, tool paths are generated in three steps. The procedure is to (1) select the tool path pattern, (2) generate tool paths over the machined area, and (3) interpolate each tool path with cutter contact points. Since

this topic has been the academic focus for decades, many approaches have been proposed. These approaches can be classified as APT method, iso-parameter, non-constant parameter, iso-cusped, orthogonal projection, and steepest-directed tree methods.

- The APT approach (APTIV) [7] was one of the earliest methods of 3-axis NC tool path planning. It positions the cutter tangent to the part surface at the cutter end and guides the cutter tangent to a series of planes. Although this method requires less computation, the tool path interval is determined subjectively and the surface roughness is not controlled.
- The iso-parametric method (Loney *et al.*, 1987, [29]; Choi *et al.*, 1988, [14], and Wysocki, 1989, [48]) retrieves from the surface iso-parametric curves, in which one surface parameter is fixed and another is varied (Mortenson, 1987, [34]) (see Fig. 1.1 above). Each iso-parametric curve is a tool path. In this work, the tool path interval is the difference between the two fixed parameters of two adjacent iso-parametric curves. The interval is set conservatively to the smallest difference between the two fixed parameters so that the highest cusp between two adjacent tool paths is equal to the surface tolerance. However, due to the non-uniform relationship between curves in parametric space and in 3D space, the tool path shape and interval are not under control (Bobrow, 1985, [5]). Thus the tool path intervals are not such determined that the cusp heights are consistent across the surface; and the cutter's machining efficiency drops in some areas.

- Huang and Oliver (1994, [22]) presented an algorithm for non-constant parameter CNC tool path generation. In this algorithm a family of parallel or non-parallel planes intersects with the surface, and the resultant intersection curves become 3-axis CNC tool paths. The plane orientation and the plane-to-plane distance affect the tool path direction and interval. Computing the tool paths in this algorithm is simple, but this algorithm is unable to improve both surface quality and tool path machining efficiency at the same time.
- The iso-cusped method was introduced by Suresh and Yang (1994, [43]) to generate 3-axis CNC tool paths that yield constant cusp heights over the machined surface. The new tool path is found by offsetting a known tool path non-uniformly so that the cusp heights between these two tool paths are equal to the specified surface tolerance. On the same track, Sarma and Dutta (1997, [38]) proposed a method to calculate the offsets according to prespecified cusp heights. The iso-cusped tool paths reduce redundant machining and produce adequate-quality surfaces.
- The research of the steepest-directed tree method was carried out at the University of Victoria by Maeng and Vickers (1996, [30]). According to the geometric features of the sculptured surface, a steepest-directed tree is constructed on a surface mesh. This tree contains all tool paths that crawl from bottom to top in the steepest way, so the tool paths have higher machining efficiency.
- Vickers and Quan (1989, [45]) deduced the cusp height as a function of the curvatures of a convex or concave surface, the cutter radius, and the path

intervals. This close-formed formula is applied on the tool path intervals when the surface tolerance, the cutter, and the surface curvature have been determined.

- Choosing the cutter contact points in each tool path or determining the step sizes is the last step in tool path planning. A simple method approximates the nominal deviation with the assumption that the point at the middle of curve parameter range is the farthest point to the chord (Wysocki *et al.*, 1989, [48]). Loney and Ozsoy (1987, [29]) found the step size by solving a polynomial equation that is obtained by imposing certain geometric constraints. Proper step sizes can reduce the over-cutting error.

1.4.3 Five-Axis CNC Tool Path Generations

The five-axis CNC tool path planning is the only way to fully use the advantages of 5-axis CNC machining centers. Unlike the 3-axis tool path pattern, the cutter orientation (A- and B-axis) in 5-axis tool paths determines the machining efficiency and avoids the surface gouging and interferences. However, automatically determining the cutter orientation has been a big challenge for some time. Many research papers have addressed this problem by optimizing the cutter orientation, gouging and inference checking, etc.

- Jenson and Anderson (1992, [23]) optimized the cutter orientation (A- and B-axis) by matching the cutting edge curvature of a flat end-mill and the maximum or minimum curvature at the cutter contact point. Mullins *et al.* (1993) extended this research from flat end-mills to torus end-mills and

developed a numerical algorithm for tool path intervals. These studies on 5-axis CNC tool paths are mainly focused on improving the cutter machining efficiency.

- Warkentin, Ismail, and Bedi (1998, [47]) proposed the multipoint machining method in which a torus end-mill machined a surface at more than one location at a time. Through geometry matching between the cutter and the surface, the cutter orientation is such determined that the cutter contacts the surface at the maximum number of points. Bedi, Gravelle, and Chen (1997, [2, 3]) introduced the principal curvature alignment method for 5-axis CNC machining.
- To address gouging of tool paths is another topic in 5-axis CNC tool path planning. Lee (1997, [26]) investigated the control of non-gouging cutter orientation along two orthogonal cutting planes in 5-axis machining, and carried out geometry analysis on surfaces machined with a torus end-mill. Lee (1998, [27]) proposed the machining strip evaluation method for 5-axis CNC tool path planning.
- Another problem in 5-axis CNC tool path planning is tool path interference checking. Interference happens when the cutter collides with the part or the fixture. Among the automatic interference checking methods, Takeuchi (1991, [44]) proposed a trial-and-error scheme through a number of provisional cutter orientations. Morishige (1997, [33]) applied the c-space concept used in robot motion planning on interference checking in order to reduce the computation.

- Suh and Lee (1998, [41, 42]) used a 3-axis CNC machine together with a rotary-tilt indexing table to machine the parts with complex shape, which usually are machined on 5-axis machine. In this method, a surface is divided into a set of sub-areas. Each sub-area is machined in its own virtual tool orientation provided by the index table. However, the number of sub-areas is determined subjectively and the cutter orientations are not optimized.

1.5 Outline of this Dissertation

This dissertation includes seven chapters covering three main parts:

- a new 3-axis CNC tool path planning principle,
- a tool path planning algorithm in 3-axis CNC machining, and
- an automated and optimized programming system for a new machining scheme as an alternative to 5-axis CNC machining.

Chapter one introduces sculptured parts, their CNC machining strategies, and the corresponding CNC tool path planning methods. The objectives of tool path planning and the problems in current tool path planning approaches are the targets in this work. Chapters two and three lay the theoretical preparation for the new 3-axis CNC tool path planning principle. The effective cutting edge is introduced, and the steepest direction is proved to be the most effective cutter feed direction. Chapter four discusses the new 3-axis CNC tool path planning principle. Chapter five applies the new principle into a new tool path generation algorithm, the integrated steepest-directed and iso-cusped tool path generation method. Chapter six addresses problems in 5-axis CNC machining. A new

machining scheme is provided as a cost-effective and industrial-applicable solution to 5-axis CNC machining. An automated and optimized programming system is established. Chapter seven contains the summary of this work.

Chapter 2 Measure of Machining Efficiency - Effective Cutting Edge

2.1 Terminology and Concepts in CNC Machining

To make this work clear and easily understood, several common terms in CNC machining are introduced. Suppose a sculptured surface on a part is machined with a torus end-mill on a 3-axis vertical CNC machine, in which the working table moves along X- and Y-axis and the cutter along Z-axis. Fig. 2.1 with a design surface and its machined surface illustrates these terms.

- A *cutter contact (CC)* point is a point on the design surface at which the cutter touches (or is tangent to) the surface in machining. The cutter machines the surface exactly at the CC points.
- A tool path of cutter contact points, briefed in this work as a *tool path*, is a curve on the design surface through a number of the CC points which the cutter passes in one successive machining (see Fig. 2.2).
- A *cutter step (motion)* is a 3D motion of the cutter moving from one CC point to the next CC point along a tool path. Thus there are many cutter steps in any tool path.

- After the cutter machines along two adjacent tool paths, some excess material is not removed between the tool paths. The ridge of excess material along the tool path is called the *cuspl curve* (see Fig. 2.1), and each point on the ridge is a *cuspl*. The distance between a cusp and the design surface is called *cuspl height*.
- The *tolerance surface* (see Fig. 2.1, [9]) is defined as an offset of the design surface by the specified surface tolerance. A qualified machined surface should lie between the design surface and the tolerance surface.
- The *machining (or cutting) efficiency* is the ratio of the amount of removed material between the tolerance and the design surface to the machining time. Specifically, provided the cutter, the cutter feed rate, and the cutter step length are fixed, the cutter removing more material in one step has higher machining efficiency, and this cutter step is more efficient.

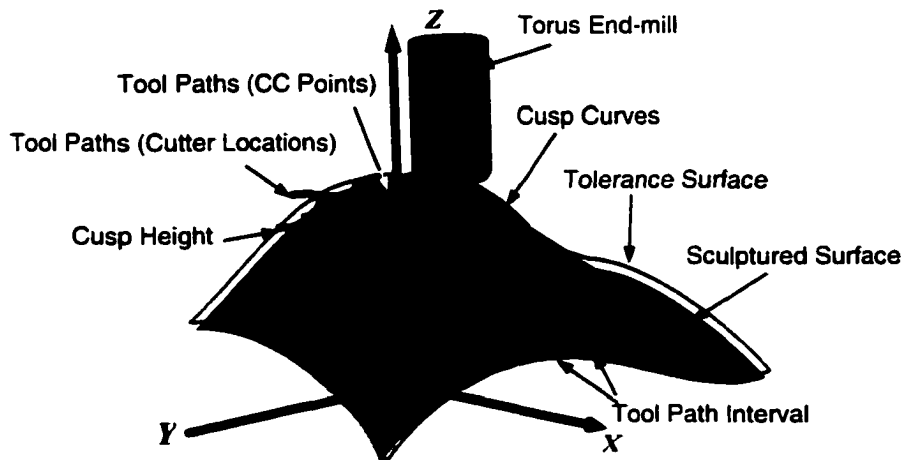


Figure 2.1 Iso-Cusped Tool Paths, Sculptured and Tolerance Surfaces

2.2 Objectives of Tool Path Planning

The ultimate goal of CNC tool path planning is to generate efficient tool paths so that the cutter can machine the sculptured part quickly and accurately. The ideal tool paths include two aspects: (1) the cutter produces a machined surface between the design surface and the tolerance surface, and all the cusps or cusp curves are on the tolerance surface; and (2) it cuts the stock material on both sides of each tool path at the maximum rate.

To plan the desired tool paths for 3-axis CNC machining, three types of information, e.g. cutter contact points, optimized tool feed directions, and tool path intervals, should be provided. Usually there are many tool paths for a sculptured surface. Machining the surface along a tool path means that the cutter moves along a tool feed direction from one CC point to the next (see Fig. 2.2). Thus, cutter contact points and tool feed direction at each point are necessary in 3-axis CNC tool path planning. In order to increase the cutting efficiency for a single tool path, the tool feed direction at each CC point should be optimized.

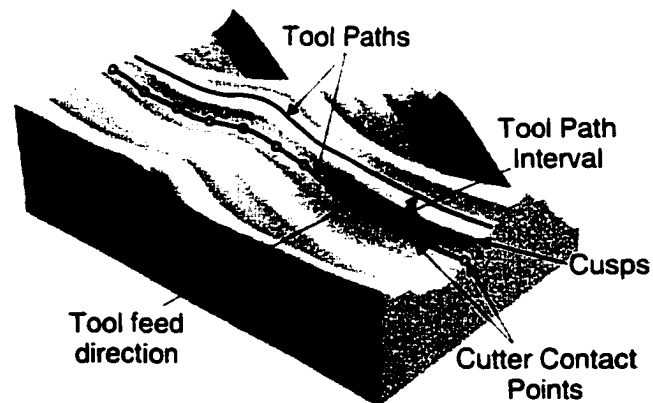


Figure 2.2 Three-Axis CNC Tool Path Diagram

between the machining efficiency and the tool feed direction (TFD). In detail, a 3-axis machining is decomposed into many tool motions or steps sequentially along each tool path. A torus end-mill with a torus-shaped cutting surface and a cylindrical cutting surface is used for general purposes (see Fig. 1.4). When the cutter moves from one CC point to another, an envelope of the torus-shaped cutting surface is generated in that step, as shown in Fig. 2.3. The cutter profile projected along the TFD on a normal plane is defined as the *planar cutting edge*. This envelope can be formed by sliding a planar cutting edge right along the TFD. All material that is above the envelope is removed, and all envelopes of the motions form a furrow along the tool path. To accurately define the furrow, a portion of the planar cutting edge between the sculptured surface and tolerance surface is called the *effective cutting edge* (ECE). The shape and the length of the ECE determine the machined surface and the cutting rate.

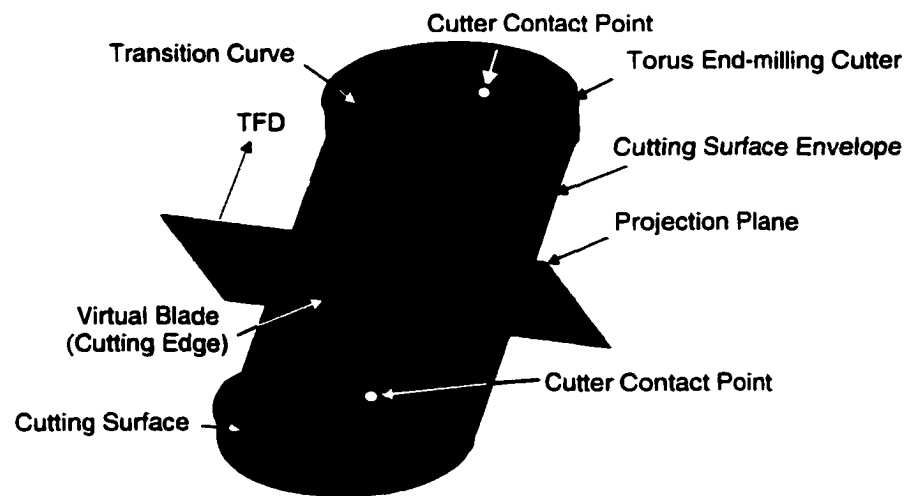


Figure 2.3 Generic Machining Model of Sculptured Parts for Effective Cutting Edge

2.4 Steepest Tangent Direction on a Sculptured Surface at a Cutter Contact Point

In this section the steepest tangent direction is introduced, and the generic formula of the steepest tangent direction on a sculptured surface is derived. Suppose a surface S in parametric form and a CC point P_0 on the surface are given in a vertical CNC machine coordinate system [20] (see Fig. 2.4), and are expressed as

$$S: \mathbf{S}(u, v) = \begin{bmatrix} x(u, v) \\ y(u, v) \\ z(u, v) \end{bmatrix} \quad (2.1)$$

$$P_0: \mathbf{P}(u_0, v_0) = \begin{bmatrix} x(u_0, v_0) \\ y(u_0, v_0) \\ z(u_0, v_0) \end{bmatrix} \quad (2.2)$$

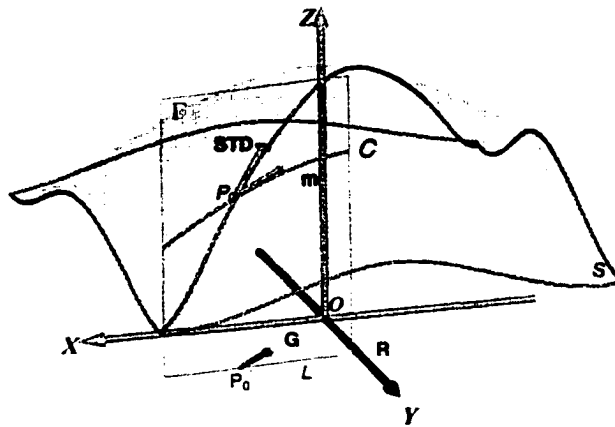


Figure 2.4 Steepest Tangent Direction of a Surface at a CC Point

This parametric form of the surface can be transformed into analytic form as $z = z(x, y)$ with the assistance of Eq. (2.3) and Eq. (2.4) [31].

$$\frac{\partial z}{\partial x} = \frac{\mathbf{D}[y, z]}{\partial(u, v)} \bigg/ \frac{\mathbf{D}[x, y]}{\partial(u, v)} \quad (2.3)$$

$$\frac{\partial z}{\partial y} = \frac{\mathbf{D}[x, z]}{\partial(u, v)} \bigg/ \frac{\mathbf{D}[x, y]}{\partial(u, v)} \quad (2.4)$$

While, $\mathbf{D}[x, y]/\partial(u, v)$, $\mathbf{D}[y, z]/\partial(u, v)$ and $\mathbf{D}[x, z]/\partial(u, v)$ are Jacobian determinants, and their forms are

$$\frac{\mathbf{D}[y, z]}{\partial(u, v)} = \begin{vmatrix} \frac{\partial y}{\partial u} & \frac{\partial z}{\partial u} \\ \frac{\partial y}{\partial v} & \frac{\partial z}{\partial v} \end{vmatrix} \quad (2.5)$$

$$\frac{\mathbf{D}[x, z]}{\partial(u, v)} = \begin{vmatrix} \frac{\partial x}{\partial u} & \frac{\partial z}{\partial u} \\ \frac{\partial x}{\partial v} & \frac{\partial z}{\partial v} \end{vmatrix} \quad (2.6)$$

$$\frac{\mathbf{D}[x, y]}{\partial(u, v)} = \begin{vmatrix} \frac{\partial x}{\partial u} & \frac{\partial y}{\partial u} \\ \frac{\partial x}{\partial v} & \frac{\partial y}{\partial v} \end{vmatrix} \quad (2.7)$$

Based on Eqs. (2.3) and (2.4), the steepest tangent direction of a surface can be derived. Project the CC point P_0 vertically onto xoy plane, and its projection is the point P_0' whose coordinates are $\mathbf{P}_0' = [x_0, y_0, z_0]^T = [x(u_0, v_0), y(u_0, v_0), 0]^T$, as shown in Fig. 2.4. Assume a free line L is crossing the point P_0' on xoy plane. Its direction is represented as the direction \mathbf{R} , which is $[a, b, 0]^T$, so the line L is formulated as

$$L: \begin{bmatrix} x \\ y \\ z \end{bmatrix} = \mathbf{P}_0' + t \cdot \mathbf{R} = \begin{bmatrix} x_0 \\ y_0 \\ 0 \end{bmatrix} + t \cdot \begin{bmatrix} a \\ b \\ 0 \end{bmatrix} = \begin{bmatrix} x_0 + at \\ y_0 + bt \\ 0 \end{bmatrix} \quad (2.8)$$

Therefore, a vertical plane passing through the line L can be defined and labelled as Γ (see Fig. 2.4). The intersection curve C between the plane Γ and the surface S can be calculated with the following group of equations:

$$\begin{cases} x = x_0 + at \\ y = y_0 + bt \\ z = z(x, y) \end{cases} \quad (2.9)$$

This intersection curve can be represented as a parametric curve of t , so the tangent of the intersection curve C at the CC point P_0 is calculated as

$$\left. \frac{\partial x}{\partial t} \right|_{P_0} = a, \quad \left. \frac{\partial y}{\partial t} \right|_{P_0} = b, \quad \text{and} \quad \left. \frac{\partial z}{\partial t} \right|_{P_0} = \left(a \cdot \frac{\partial z}{\partial x} + b \cdot \frac{\partial z}{\partial y} \right) \Big|_{P_0} \quad (2.10)$$

A vector \mathbf{m} aligning with the tangent direction is simply denoted by the form below, and this vector is the tool feed direction.

$$\mathbf{m} = \left[a, \quad b, \quad a \cdot \frac{\partial z}{\partial x} + b \cdot \frac{\partial z}{\partial y} \right]^T \quad (2.11)$$

On the other hand, the directional derivative and gradient formula can be deduced based on computational geometry [34]. For the surface S with analytic form, $z = z(x, y)$, its gradient \mathbf{G} at the CC point is $[\partial z/\partial x, \partial z/\partial y, 0]^T$, and the direction derivative of the surface function, $z = z(x, y)$, along the direction \mathbf{R} is computed in Eq. (2.12).

$$|\nabla z| = \mathbf{G}^T \cdot \mathbf{R} = \begin{bmatrix} \frac{\partial z}{\partial x} & \frac{\partial z}{\partial y} & 0 \end{bmatrix} \cdot \begin{bmatrix} a \\ b \\ 0 \end{bmatrix} = a \cdot \frac{\partial z}{\partial x} + b \cdot \frac{\partial z}{\partial y} \quad (2.12)$$

Comparing Eqs. (2.10) and (2.12), the directional derivative of the surface along the direction \mathbf{R} equals the z component of the tool feed direction \mathbf{m} . The directional derivative physically means the projection of the surface gradient \mathbf{G} at the CC point P_0 to the direction \mathbf{R} . The z component of the tool feed direction \mathbf{m} reflects the slope of the direction.

From geometric projection point of view, the directional derivative reaches the maximum when the free direction \mathbf{R} is in line with the gradient \mathbf{G} , $\mathbf{R} = \mathbf{G} = [\partial z/\partial x, \partial z/\partial y, 0]^T$. The maximum directional derivative is $|\nabla z| = (\partial z/\partial x)^2 + (\partial z/\partial y)^2$. In this case, the z component of the tool feed direction is the maximum; therefore, the tool feed direction is the steepest. The *steepest tangent direction* can thus be obtained. When rotating the plane Γ along the axis P_0P_0' from a direction \mathbf{R} to the surface gradient \mathbf{G} , the intersection curve C between the plane Γ and the surface S is changed accordingly. When the direction \mathbf{R} is aligned with the surface gradient \mathbf{G} , the tool feed direction \mathbf{m} becomes the steepest tangent direction (**STD**) at the CC point P_0 (see Fig. 2.4). Thus, the **STD** on a surface $z = z(x, y)$ at the CC point P_0 is formulated as

$$\mathbf{SD} = \left[\frac{\partial z}{\partial x}, \frac{\partial z}{\partial y}, \left(\frac{\partial z}{\partial x} \right)^2 + \left(\frac{\partial z}{\partial y} \right)^2 \right]^T \quad (2.13)$$

For a sculptured surface in 3-D space, there exists only one steepest tangent direction at any point on the surface. This formula is also applicable to a sculptured surface in a horizontal CNC machine coordinate system, where the z -axis is in horizontal direction.

2.5 Cutter and Surface Normal Expressions in Cutter Motion Frame

To find the mathematic formulae of the planar cutting edge and the ECE length, four frames or Cartesian coordinate systems are built to facilitate the projection of a torus end-mill along the TFD. The frames include *cutter geometry frame* (CGF), *cutter location frame* (CLF), *steepest direction frame* (SDF), and *cutter motion frame* (CMF). Because of the position relationships between each pair of the successive frames, the cutter and the surface normal expressions in the CGF can be transformed sequentially [51] through the CLF, the SDF, into the CMF, in which the cutter projection is easily obtained.

2.5.1 Cutter Geometry Frame (CGF)

Assume a sculptured surface S in the world coordinate system is cut by a torus end-mill at a CC point P_0 on a 3-axis vertical CNC machine (see Fig. 2.3). In this machine configuration, the cutter axis is in the direction $[0 \ 0 \ 1]^T$. Cutter geometry frame (i-j-k) is built in such a way that its origin is at the cutter tip; its k-axis is aligned with the cutter axis; and its i-axis is on the plane spanned by the k-axis and the surface normal n at the CC point, pointing away from the surface (see Fig. 2.5). The expression of the torus-shaped cutting surface in the CGF is Eq. (2.14).

$$\begin{bmatrix} i \\ j \\ k \end{bmatrix} = \begin{bmatrix} (R_1 + R_2 \cdot \sin \varphi) \cdot \cos \theta \\ (R_1 + R_2 \cdot \sin \varphi) \cdot \sin \theta \\ R_2 \cdot (1 - \cos \varphi) \end{bmatrix} \quad (2.14)$$

where $R_1 > 0$, $R_2 > 0$ and $R_1 \gg R_2$; $\varphi \in [0, \frac{\pi}{2}]$ and $\theta \in [0, 2\pi]$. The mill parameters are labelled in Fig. 2.6.

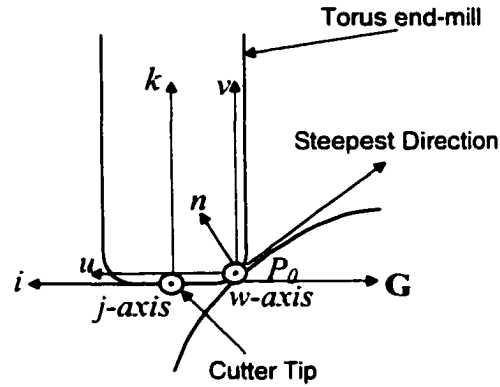


Figure 2.5 Torus End-mill in Cutter Geometry Frame and Cutter Location Frame

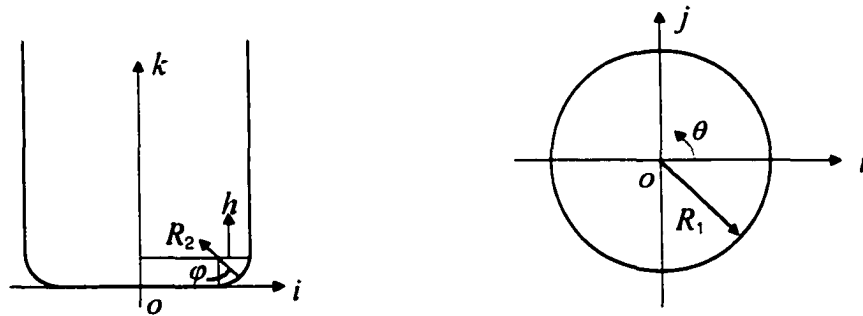


Figure 2.6 Torus End-mill Diagram

The cylindrical cutting surface is represented as

$$\begin{bmatrix} i \\ j \\ k \end{bmatrix} = \begin{bmatrix} (R_1 + R_2) \cdot \cos \theta \\ (R_1 + R_2) \cdot \sin \theta \\ R_2 + h \end{bmatrix} \quad (2.15)$$

For P_0 , its parameter θ is π . If its parameter φ is assumed to be φ_0 , its coordinate in the CGF is $[-(R_1 + R_2 \sin \varphi_0), 0, R_2(1 - \cos \varphi_0)]^T$.